PAPER

Accumulation of camptothecin and 10-hydroxycamptothecin and the transcriptional expression of camptothecin biosynthetic genes in *Camptotheca acuminata* cambial meristematic and dedifferentiated cells

Yuhua Zhang,[abc] Keming Jiang,[a] Degang Qing,[d] Bing Huang,[a] Jiayi Jiang,[a] Shumei Wang*[bc] and Chunyan Yan*[a]

Camptotheca acuminata Decne (Nyssaceae) is a major natural source of the anticancer drug camptothecin (CPT) and its derivatives. The leaves and stems are two of the main regions that accumulate CPT in *C. acuminata*. In this study, we successfully isolated cambial meristematic cells (CMCs) and dedifferentiated cells (DDCs) from *C. acuminata* stems and leaves, identified their characteristic features using micrograph analysis, and assessed their hypersensitivity to γ-irradiation and zeocin. The growth and kinetics curves of CMCs and DDCs were also studied. Furthermore, the accumulation of CPT and 10-hydroxycamptothecin (HCPT)—a more potent and less toxic CPT derivative—was assessed by liquid chromatography, and the transcriptional levels of nine genes encoding key enzymes involved in CPT and HCPT biosynthesis was assessed using quantitative real-time polymerase chain reaction (PCR) in CMCs and DDCs. The results showed that CMCs induced were particularly hypersensitive to γ-irradiation and zeocin and presented with abundant and small vacuoles, whereas DDCs were not. The above morphological and physiological characteristics of CMCs were consistent with previous reports. B_5 medium was determined as the best growth medium for CMCs and DDCs. The accumulation of CPT and HCPT was higher in CMCs than DDCs, and the expression of *IPI*, *G10H*, *ASA1*, *TSB*, *TDC1*, *TDC2*, and *STR* was significantly upregulated in CMCs compared with DDCs; *HMGR2* and *HMGR3* were downregulated in CMCs. We speculate that the high accumulation of CPT and HCPT in CMCs was due to the upregulation of these seven genes.

Introduction

Camptotheca acuminata Decne belongs to the family of Nyssaceae and genus *Camptotheca*, and can produce camptothecin (CPT).[1] CPT is a terpenoid indole alkaloid (TIA) that exhibits anti-cancer activity by inhibiting DNA topoisomerase I to kill cancer cells.[2] However, CPT was not directly used in clinical treatment because of negligible water solubility and severe side effects according to a previous report.[3] Conversely, 10-hydroxycamptothecin (HCPT) has been used for clinical research and was approved by the State Food and Drug Administration (SFDA) of China in 2002. In addition, CPT and HCPT are chemical precursors of anticancer drugs such as topotecan and irinotecan, which were approved for the treatment of cervical cancer, ovarian cancer, small-cell lung cancer, and metastatic colorectal cancer by the United States Food and Drug Administration (FDA) in 1994.[4] Practically, soil-grown *C. acuminata* are not only restricted by limited natural resources and the environment, but also produce only 0.2–5.0 mg g^{-1} dry-weight (DW) CPT in the whole plant and 2–90 μg g^{-1} DW HCPT in the bark. This illustrates a serious resource crisis that should be alleviated using various approaches to identify alternative sources of CPT and HCPT.[5] Sakato *et al.* first performed studies of *C. acuminata* cell culture, which produced 2.5 μg g^{-1} DW CPT.[6] Callus cultures of *C. acuminata* produced 1–2 mg g^{-1} DW CPT and 80–100 μg g^{-1} DW HCPT.[7,8] Later, some studies were performed to improve CPT production in *C. acuminata*. *C. acuminata* seedlings treated with elicitors such as abscisic acid (ABA), methyl jasmonate (MeJA), and salicylic acid (SA) produced 1.33–1.81 mg g^{-1} DW CPT and 2.25–2.60 mg g^{-1} DW HCPT.[9] Hairy roots of *C. acuminata* induced by *Agrobacterium rhizogenes*

a School of Pharmacy, Guangdong Pharmaceutical University, Guangzhou 510006, China. E-mail: ycybridge@163.com; Fax: +86-20-39352052; Tel: +86-20-39352052

b Key Laboratory of Digital Quality Evaluation of Chinese Materia Medica of State Administration of TCM, P. R. China

c Engineering & Technology Research Center for Chinese Materia Medica Quality of the Universities of Guangdong Province, China

d XinJiang Institute of Chinese Materia Medica and Ethnodrug, Urumqi 830002, China

produced 1.0–1.2 mg g^{-1} DW CPT and 0.15–0.31 mg g^{-1} DW HCPT.[3,10,11]

Several attempts have been made to improve the production of CPT, as mentioned above. However, no relevant studies of cultured cambial meristematic cells (CMCs) from *C. acuminata* have been reported. CMCs are innately undifferentiated cells located in the meristems of plants; they circumvent the dedifferentiation process and serve as the origin of plant vitality.[12,13] CMCs are not negatively restricted by the source of the plant, the location, the season of harvest, and the prevailing environmental conditions; therefore, they alleviate the pressure on limited wild plant resources.[12] Compared with dedifferentiated cells (DDCs) suspension cultures, CMCs suspension cultures can tolerate shear stress and thereby avoid cell aggregation in air-lift bioreactors for small or large-scale cultures because of the presence of small, abundant vacuoles within each CMC; they can also maintain a stable constant growth rate on an industrial scale.[13–15] CMCs can also secrete more natural products into the medium than DDCs. For example, the CMCs of *Taxus cuspidata* secrete 102 mg kg^{-1} fresh cell weight paclitaxel after culture for 10 days, whereas DDCs induced from *T. cuspidata* secrete just 23 mg kg^{-1} and 39 mg kg^{-1}, respectively.[13] Accordingly, CMCs are not only completely suitable for use in industrial production but also yield natural plant products.

In this study, *C. acuminate* CMCs were induced for the first time, and their morphological and physiological characteristics were consistent with CMCs previously reported.[13] We then evaluated the accumulation of CPT and HCPT by liquid chromatography (HPLC) and investigated the expression of nine genes in CMCs and DDCs from *C. acuminate* using quantitative real-time PCR (qRT-PCR). Our results are expected to provide a new promising culture method to improve the content of CPT and its derivatives and thereby develop a sustainable method of obtaining CPT and HCPT in the future.

Results and discussion

Induction of CMCs and DDCs

For CMCs, cambium, phloem, cortex, and epidermal stem tissues were peeled off from the xylem and laid on MS medium (Fig. 1A). After 10 days, the cambium started to present evident cell division. However, the phloem, cortex, and epidermis started to exhibit cell division by dedifferentiation by 21 days. After 60 days, compared with dim and irregular cells in phloem, cortex, and epidermal (black arrow), there were some white and loose proliferating cells in the cambium, which were CMCs (red arrow), and a visible split was observed between them (Fig. 1B). A pair of tweezers was used to gently separate the CMCs from the dim and irregular cells in the phloem, cortex, and epidermis. And the CMCs and dim and irregular cells were transferred to Murashige and Skoog (MS) medium supplemented with 0.1 mg L^{-1} 2,4-dichlorophenoxyacetic acid (2,4-D), 0.1 mg L^{-1} kinetin (KT), and 0.1 mg L^{-1} naphthalene-acetic acid (NAA). The CMCs of a variety of plant species, including *T. cuspidate*, *Panax ginseng*, *Ginkao biloba*, and *Solanum lycopersicon*, have been obtained using the above technology.[13] After subculture seven times, the phloem, cortex, and epidermal
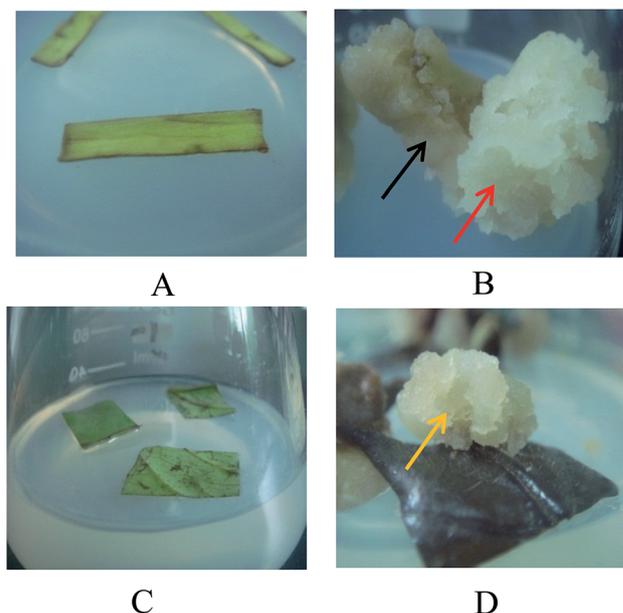

Fig. 1 The induction and isolation of CMCs and DDCs from *C. acuminata*. (A) Cambium, phloem, cortex, and epidermal tissues from *C. acuminata* were laid on solid MS medium. (B) There was a visible split between CMCs (red arrow) and DDCs (black arrow). (C) *C. acuminata* leaves were laid on MS medium. (D) A mass of DDCs (yellow arrow) proliferated from the leaves.

cultures were brown and dead. In contrast, the CMCs were in good condition.

For DDCs, wounded leaves were laid on MS medium (Fig. 1C), and cell division appeared in the wounds by dedifferentiation to produce many proliferating cell masses. After 65 days, the actively growing cells were gently separated from the explants and cultured in new MS medium supplemented with 0.1 mg L^{-1} 2,4-D, 0.1 mg L^{-1} KT, and 0.1 mg L^{-1} NAA (Fig. 1D, yellow arrow).

Identification of CMCs and DDCs

Observed under an optical microscope, single CMC presented with abundant and small vacuoles, which is the notable characteristic feature of CMCs (Fig. 2A).[12] However, single DDC just had a large vacuole (Fig. 2B). Treating with 0.1% neutral red stained the vacuoles red, there were abundant and small red vacuoles in single CMC (Fig. 2C) compared with a large red vacuole in single DDC (Fig. 2D). The above properties of the CMCs obtained from *C. acuminata* are characteristic of cambium stem cells.[13,15]

CMCs and DDCs were observed and photographed under a fluorescent inverted microscope after treatment with different doses of γ-irradiation and incubation for 24 h in the dark. Thereafter, images were processed by Adobe Photoshop software (Fig. 3A1–A3 and B1–B3). Fig. 4C shows that the cell death rate was significantly higher in CMCs than DDCs after treatment with different doses of γ-irradiation ($P < 0.05$). After incubation for 24 h in the dark, the cell death rate of CMCs gradually increased with increasing doses of γ-irradiation
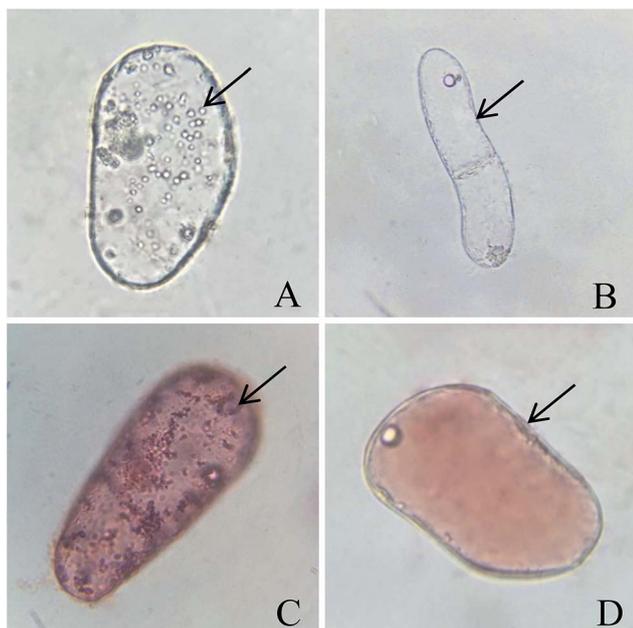
Fig. 2 Micrographs of CMCs and DDCs from *C. acuminata*. The vacuole is indicated using a black arrow. Micrographs of single CMC (A) and DDC (B). Micrographs of single CMC (C) and DDC (D) after stained with neutral red.

(40–200 Gy), and reached 72.1% with 200 Gy. However, DDCs cell death reached only 31.1% after exposure to 200 Gy of γ-irradiation. These results suggest that CMCs were significantly more sensitive to γ-irradiation than DDCs.

CMCs and DDCs were incubated with different concentration zeocin for 24 h in the dark, and then photographed (Fig. 4A1–A3 and B1–B3). The cell death rate of CMCs was increased significantly ($P < 0.05$) compared with that of DDCs treated with different concentrations of zeocin, as shown in Fig. 5C. After incubation in medium containing 40 μg mL^{-1} zeocin for 24 h, CMCs had a high death rate of 80.5%. The cell death rate of CMCs had little increase at doses of 80–200 μg mL^{-1} zeocin, and reached 82.8% with 200 μg mL^{-1}. However, the maximum DDCs death rate was 35.1% after incubation with different concentrations of zeocin for 24 h. These results suggest that CMCs were particularly hypersensitive to zeocin, whereas DDCs were not.

The morphologic and physiologic characteristics of CMCs, including microscopic analysis revealing small, abundant vacuoles, hypersensitivity to γ-irradiation and the radiomimetic drug zeocin, and increased cell death rates, have been analyzed in a variety of plant species.[12–16] The above traits of CMCs from *C. acuminate* are completely consistent with the CMCs reported previously.

Optimization of the growth medium for CMCs and DDCs

To optimize the growth medium, CMCs and DDCs were subcultured in MS, B$_5$, BDS, or SH medium supplemented with 0.1 mg L^{-1} 2,4-D, 0.1 mg L^{-1} 6-benzyl aminopurine (6-BA), and 30 g L^{-1} sucrose. After 36 days, the dry weight of the cultures was used to establish growth curves, which were made up of the lag phase, the logarithmic phase, and the plateau phase. For CMCs, B$_5$ was obviously the best choice of growth medium. The logarithmic phase of cultures occurred at days 12–24. Thereafter, the growth of the cultures entered the plateau phase. Ultimately, the cultures had a total DW of 5.0 ± 0.8 g L^{-1} in the plateau phase, which was an approximate 6.3-fold increase compared with the DW at day 3 (Fig. 5A). For DDCs, cultures grown in SH medium had a better growth state, with a logarithmic phase at days 9–15 (Fig. 5B). However, the growth of DDCs decreased slowly after subculture some times. As a result, B$_5$ medium was selected as the growth medium for DDCs. Ultimately, B$_5$ medium supplemented with 1.0 mg L^{-1} NAA, 0.5 mg L^{-1} 2,4-D, 0.05 mg L^{-1} KT, and 30 g L^{-1} sucrose was used as the subculture medium for both CMCs and DDCs, and the cells were subcultured every 21 days.

The growth kinetics of CMCs and DDCs

According to the sucrose, PO_4^{3-}, NH_4^+ and NO_3^- content in the media and pH of media, additional information was obtained about the CMCs and DDCs from *C. acuminata*. The consumption of sucrose was consistent with the logarithmic phase of the cultures. Sucrose, which is used as the energy source for cell division, was quickly consumed when the cultures were about to enter the logarithmic phase after 6 days in culture in both CMCs and DDCs (Fig. 5C). Sucrose was consumed slowly when the cultures entered the plateau phase. Phosphorus is a constituent of membrane phospholipids and nucleic acids, and was consumed quickly when CMCs and DDCs were subcultured for 6–15 days (Fig. 5D). The pH of the media fluctuated between 5.0–7.0 during the growth period in both CMCs and DDCs (Fig. 5D). Ammonium and nitrate were immediately utilized to synthesis proteins when CMCs and DDCs were cultured (Fig. 5E). The nitrate content in the medium was stable after CMCs and DDCs were cultured for 21 days. However, ammonium levels were ultimately almost exhausted at the end of the plateau phase in both CMCs and DDCs. This demonstrates that the subculture media had a good buffering capacity and satisfied the demands for sucrose, phosphorus, ammonium, and nitrate during the growth of CMCs and DDCs.

Quantification of CPT and HCPT

CPT and HCPT have anti-cancer activity, and are used for the treatment of a diverse range of cancers.[2,3] CPT and HCPT were detected in both CMCs and DDCs from *C. acuminata*. The concentration of CPT in CMCs (2.55 μg g^{-1} DW) was 1.55-fold higher than that in DDCs (1.65 μg g^{-1} DW). Similarly, the concentration of HCPT in CMCs (25.59 μg g^{-1} DW) was 2.50-fold higher than that in DDCs (10.22 μg g^{-1} DW). Significantly, CMCs from *C. acuminata* were capable of yielding more CPT and HCPT than DDCs.

Expression of CPT and HCPT biosynthesis genes

The CPT and HPCT biosynthesis pathway in *C. acuminata* is a very complex process that involves many vital steps that are controlled by the key enzymes isopentenyl diphosphate
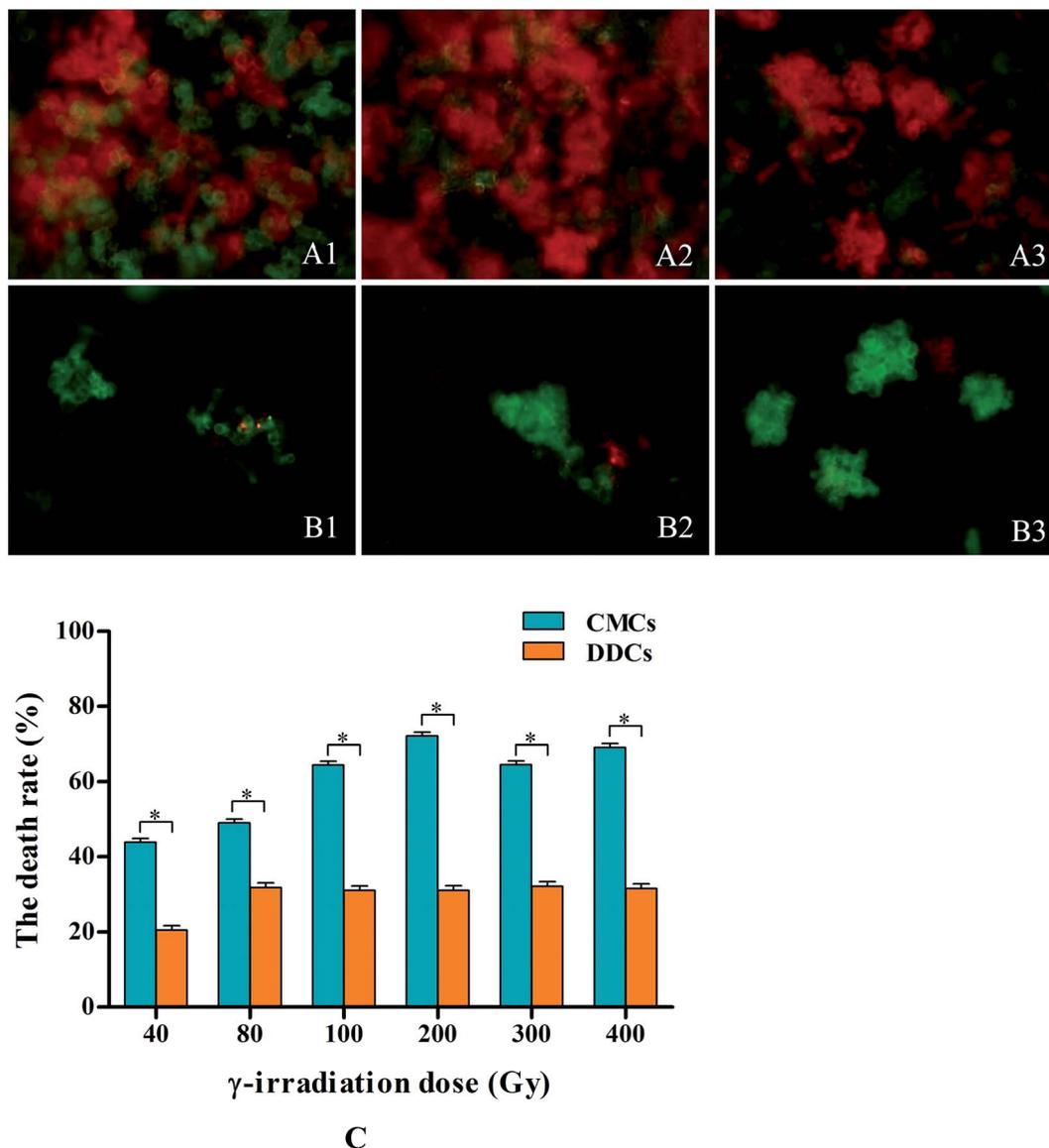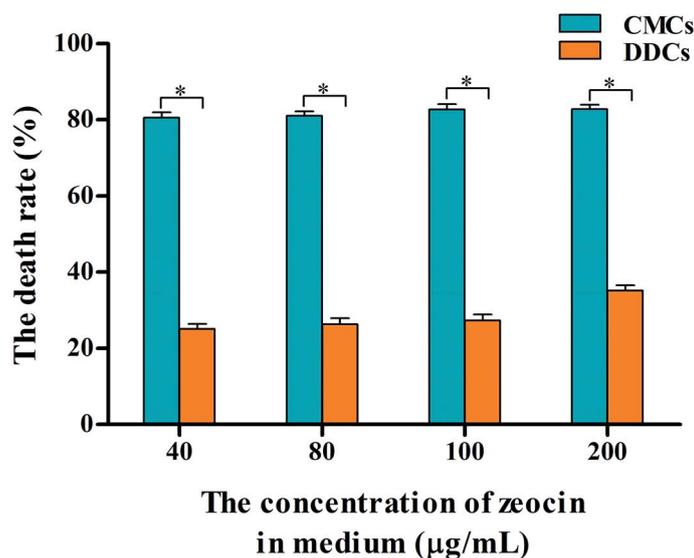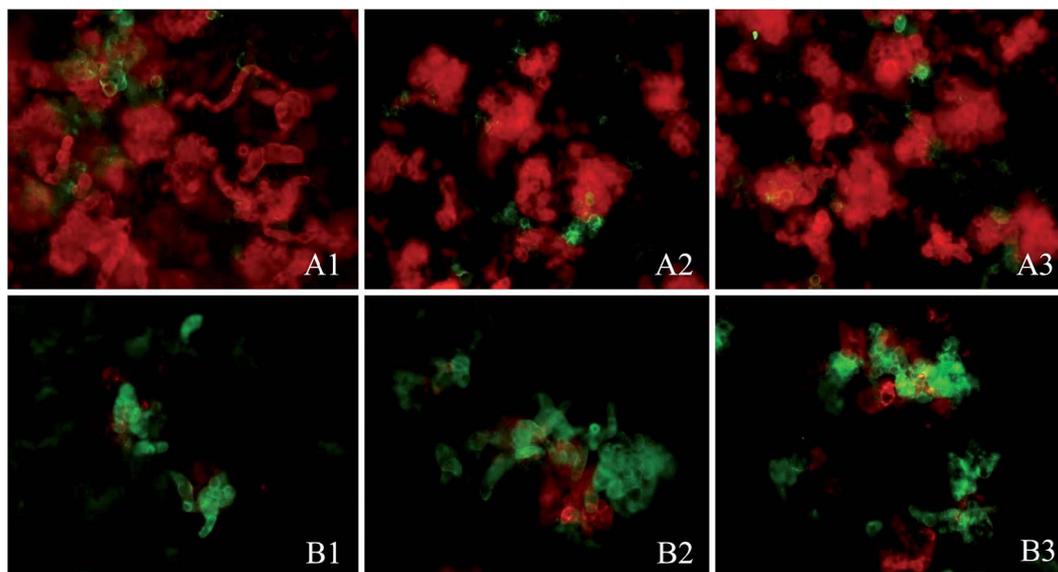
Fig. 3 Effects of γ-irradiation on the death of *C. acuminata* CMCs and DDCs. Values are expressed as means ± SDs ($n = 3$), *$P < 0.05$. Micrographs of CMCs (A1–A3) and DDCs (B1–B3) incubated for 24 h in the dark after exposure to γ-irradiation. Bright green fluorescence indicates live cells, and bright red fluorescence indicates dead cells. (C) The death rates of CMCs and DDCs after exposure to different dose of γ-irradiation and incubation for 24 h.

isomerase (IPI), geraniol-10-hydroxylase (G10H), anthranilate synthase (ASA), tryptophan synthase (TSB), tryptophan decarboxylase (TDC), strictosidine synthase (STR), and 3-hydroxy-3-methylglutaryl-CoA reductase (HMGR) (Fig. 6). The genes encoding the above enzymes have all been isolated from *C. acuminata*.[17–23] To gain insight into the molecular events underlying the significant difference between CPT and HCPT concentrations in CMCs and DDCs, the transcriptional expression of *IPI*, *G10H*, *ASA1*, *TSB*, *TDC1*, *TDC2*, *STR*, *HMGR2* and *HMGR3* was monitored using qRT-PCR (Fig. 7). The relative expression levels of *HMGR2*, *HMGR3*, *TSB*, *TDC1*, *TDC2*, and *STR* were normalized to the reference housekeeping gene *actin* as an internal standard. In contrast, the relative expression levels of *IPI*, *G10H*, and *ASA1* were normalized to the reference

housekeeping gene *18S* as the internal standard. The expression levels of *IPI*, *G10H*, *ASA1*, *TSB*, *TDC1*, *TDC2*, *STR*, *HMGR2*, and *HMGR3* were significantly different between CMCs and DDCs ($P < 0.01$, $P < 0.001$, $P < 0.001$, $P < 0.01$, $P < 0.05$, $P < 0.05$, $P < 0.001$, $P < 0.01$, and $P < 0.001$, respectively). The expression of *IPI*, *ASA1*, *TSB* and *TDC1* were significantly higher in CMCs, with a 1.99-, 1.80-, 1.78-, and 1.47-fold increase compared with DDCs, respectively. The expression levels of *TDC2* and *G10H* were 4.56- and 4.07-fold higher in CMCs compared with DDCs, respectively. In particular, the expression of *STR* was 8.86-fold higher in CMCs than DDCs. In contrast, *HMGR2* and *HMGR3* levels were 2.51- and 4.28-fold higher in DDCs compared with CMCs, respectively.

Fig. 4 Effects of zeocin on the death of *C. acuminata* CMCs and DDCs. Values are expressed as means ± SDs ($n = 3$), *$P < 0.05$. Micrographs of CMCs (A1–A3) and DDCs (B1–B3) after incubation in medium containing zeocin for 24 h in the dark. (C) The death rates of CMCs and DDCs after incubation in medium containing different concentration of zeocin for 24 h.

Obviously, the transcriptional expression of *IPI*, *G10H*, *ASA1*, *TSB*, *TDC1*, *TDC2* and *STR* in CMCs was remarkably upregulated, whereas *HMGR2* and *HMGR3* were not. The effects of the expressions of the above genes on terpenoid synthesis have been reported. For example, Kajiwara *et al.* reported that expression of *IPI* could enhance isoprenoid biosynthesis in *Escherichia coli*.[24] The co-overexpression of *G10H* and *1-deoxy-D-xylulose synthase* (*DXS*) or *ASA* and *DXS* resulted in an increase in several TIAs in *Catharanthus roseus* hairy roots.[25] It was also reported that the G10H activity was correlated to the accumulation of TIAs in *C. roseus*.[26] The patterns of *STR* expression

roughly correlated with CPT accumulation in some organs of *Ophiorrhiza pumila*.[27] HMGR catalyzes the conversion of 3-hydroxy-methylglutaryl-CoA (HMG-CoA) to mevalonate (MVA), and this conversion is the first key step in the MVA pathway in plants. In addition, the *HMGR* gene plays a key role in the biosynthesis of triterpenoid in many medical plants, and its overexpression can improve the production of triterpenoid.[28–30] We speculate that the high accumulation of CPT and HCPT in CMCs could likely be attributed to the effects of the upregulation of the above mentioned seven genes, which offset the downregulation of *HMGR2* and *HMGR3*.
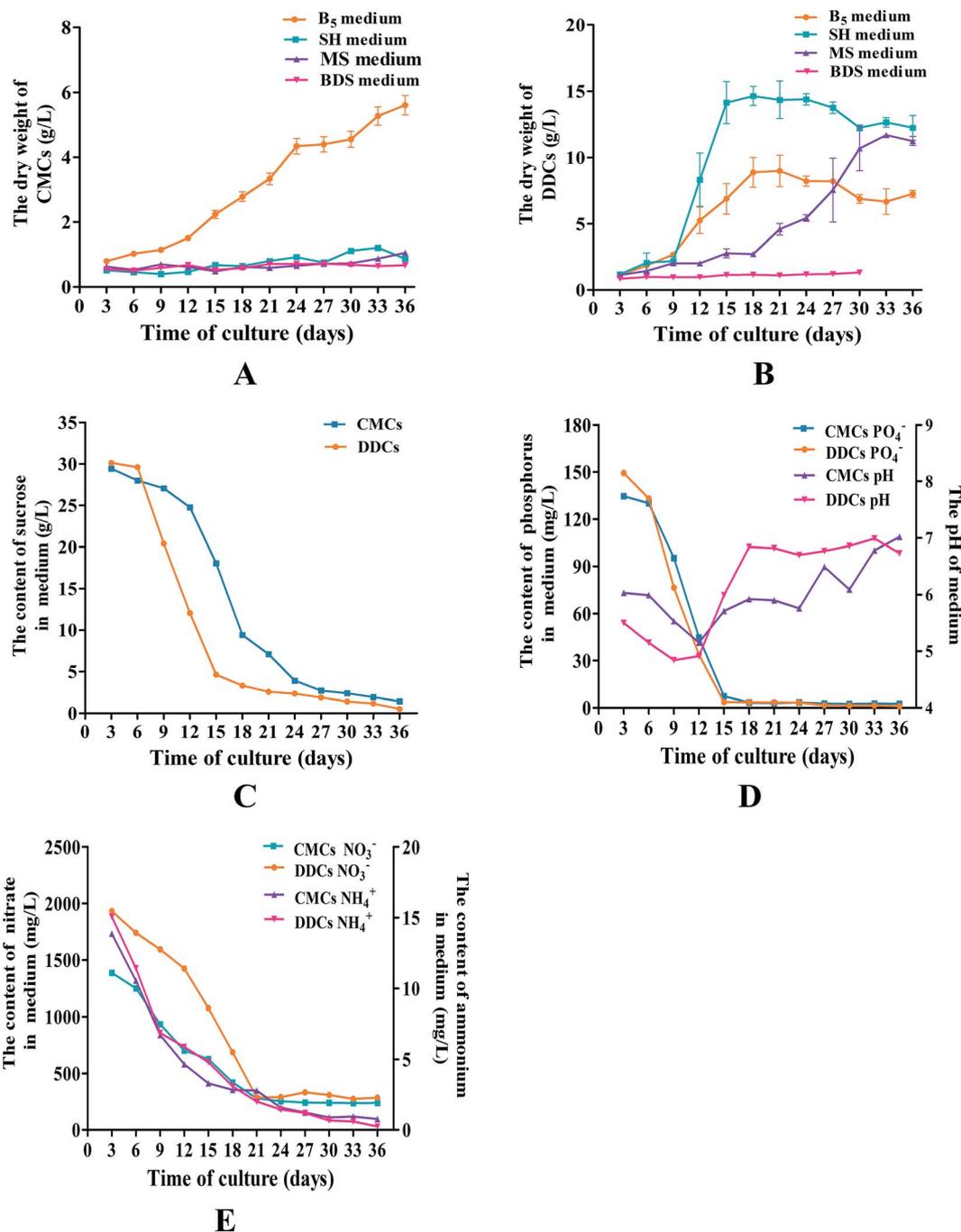
Fig. 5 The growth curves and kinetics of CMCs and DDCs from *C. acuminata*. Values are expressed as means ± SDs ($n = 3$). The dry weight of CMCs (A) and DDCs (B) from *C. acuminata* on MS, B_5, BDS, or SH medium. (C) Time course of the sucrose content in medium containing CMCs and DDCs. (D) Time course of the phosphorus content and pH of medium containing CMCs and DDCs. (E) Time course of the nitrate and ammonium content of medium containing CMCs and DDCs.

Experimental

Induction of CMCs and DDCs

The stems and leaves of *C. acuminata* were obtained from Yaowang Mountain, Guangzhou University of Chinese Medicine, Guangzhou, China. The stems were washed immediately in running tap water for 30 min, and the surfaces were disinfected with 75% ethanol for 1 min. They were then washed with sterilized distilled water (dH_2O), before 1% NaOCl and a drop of Tween-20 were added, and mixed vigorously for 4 min. After an additional wash with dH_2O, 0.1% $HgCl_2$ and a drop of Tween-20 were added, and the stems were mixed vigorously for 4 min and washed with dH_2O. The leaves were sterilized as described above, but were maintained in $HgCl_2$ for only 2 min due to their tender nature.
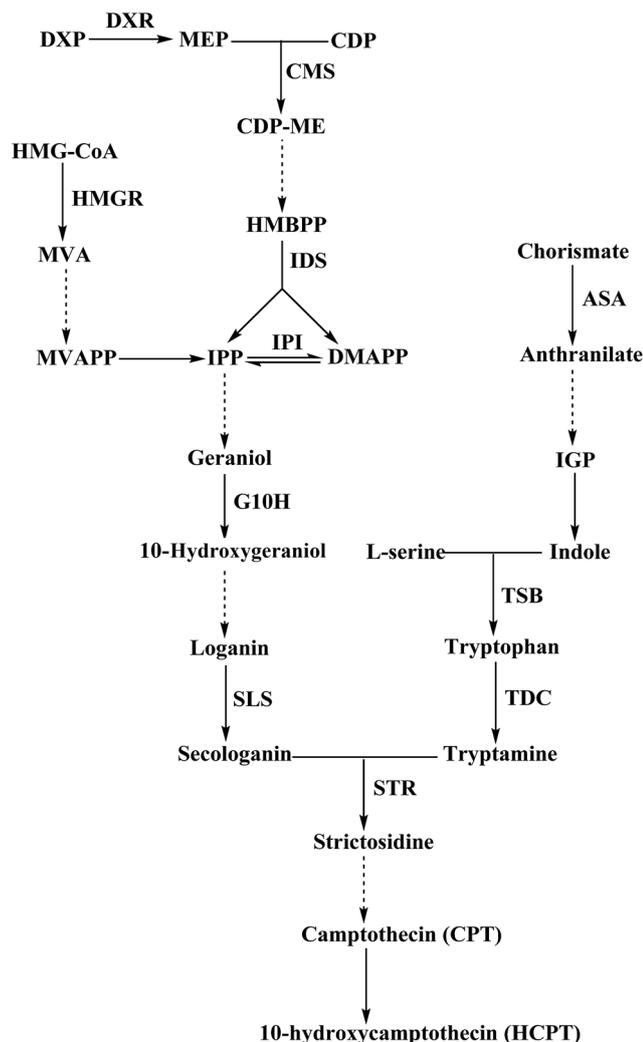
Fig. 6 Biosynthesis pathway of CPT and HCPT. Dotted line arrows indicated the involvement of multiple enzymatic steps. DXR, DXP reductoisomerase; CMS, 4-(cytidine 5-diphospho)-2-C-methylery-thritol synthase; IDS, IPP/DMAPP synthase; IPI, IPP isomerase; HMGR, 3-hydroxy-3-methylglutaryl-CoA reductase; G10H, geraniol-10-hydroxylase; SLS, secologanin synthetase; ASA, anthranilic acid synthetase; TSB, tryptophan synthase beta; TDC, tryptophan decarboxylase; STR, strictosidine synthase.

Fig. 7 The relative expression levels of *IPI*, *G10H*, *ASA1*, *TSB*, *TDC1*, *TDC2*, *STR*, *HMGR2*, and *HMGR3* in CMCs and DDCs. Three replicates per sample were used for qRT-PCR, and the values are expressed as means ± SDs ($n = 3$). *$P < 0.05$, **$P < 0.01$, and ***$P < 0.001$.

For CMCs, stems were cut into 1 cm (length) segments. The cambium, phloem, cortex, and epidermal tissue were peeled off from the xylem and laid on 100 mL Erlenmeyer flasks containing 40 mL of MS medium supplemented with 0.1 mg L^{-1} 2,4-D, 0.1 mg L^{-1} KT, 0.1 mg L^{-1} NAA, and 30 g L^{-1} sucrose. The pH of the medium was adjusted to 5.75 before the addition of 7.5 g L^{-1} agar, which was followed by sterilization at 121 °C for 20 min. The explants were cultured at 25 ± 1 °C in the dark. For DDCs, leaves were cut and laid on MS medium as described above.

Identification of CMCs and DDCs

Micrographs of CMCs and DDCs. DDCs and CMCs were treated with 0.1% neutral red (Aladdin, Shanghai, China) for 10 min, rinsed with phosphate buffer (pH 6.5) several times,
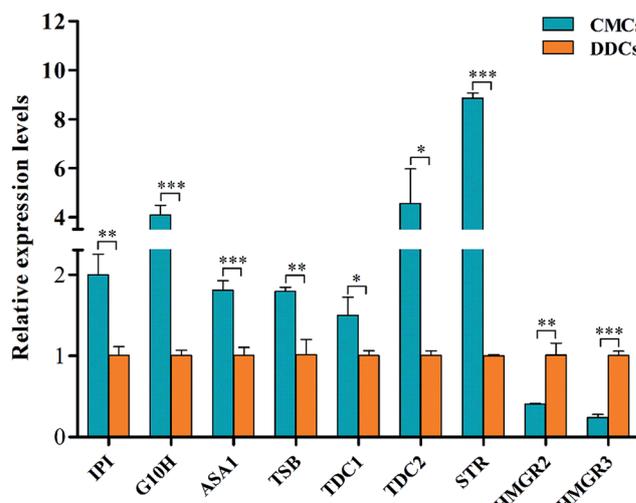
and then observed under an optical microscope (ML32, MSHOT, China).

Influence of γ-irradiation and zeocin on CMCs and DDCs. CMCs and DDCs suspension cells were obtained after culture for 15 days. For γ-irradiation treatments, cultures were irradiated with 40, 80, 100, 200, 300, and 400 Gy at a dose rate of 2.67 Gy min^{-1}, and placed back in culture at 25 °C in the dark for 24 h. For zeocin treatments, cultures were placed in medium containing 40, 80, 120, and 200 μg mL^{-1} zeocin (Invitrogen, Carlsbad, USA), and agitated at 110 rpm at 25 °C in the dark for 24 h. To detect cell death, cells were treated with a fluorescent dye containing 0.1% fluorescein diacetate (FDA; Sigma, USA) and 0.1% Evan's blue (EB; Sigma) for 10 min, rinsed with phosphate buffer several times, and transferred to a Petri dish. Then, FDA and EB were excited using red and blue ion lasers under a fluorescent inverted microscope (BX43, Olympus, Japan) as previously described.[14] The number of stained living (green) and dead (red) CMCs and DDCs was counted and the cells were photographed under the same view using a fluorescent inverted microscope. Three different fields were analyzed in each group.

Optimizing the growth medium for CMCs and DDCs

CMCs and DDCs were inoculated into 250 mL Erlenmeyer flasks containing 80 mL of MS, B_5, BDS, or SH medium supplemented with 0.1 mg L^{-1} 2,4-D, 0.1 mg L^{-1} 6-BA, and 30 g L^{-1} sucrose. The Erlenmeyer flasks were agitated at 110 rpm and 25 °C in the dark. Cultures were assessed every 3 days to day 36 to establish growth curves. All cultures were analyzed in triplicate, and the values are expressed as means ± SDs.

The growth kinetics of CMCs and DDCs

According to the CMCs and DDCs growth curves obtained in different media described in Section 2.3, both CMCs and DDCs

were inoculated into 250 mL Erlenmeyer flasks containing 80 mL B_5 medium supplemented with 0.1 mg L^{-1} 2,4-D, 0.1 mg L^{-1} 6-BA, and 30 g L^{-1} sucrose. The Erlenmeyer flasks were agitated at 110 rpm and 25 °C in the dark. Liquid cultures were removed every 3 days to day 36 to study the growth kinetics of CMCs and DDCs. After the liquid media were filtered, the sucrose, NH_4^+, NO_3^- and PO_4^{3-} contents in the filtrate were measured using phenol–sulfuric acid, phenol–hypochlorite, salicylic acid–sulfuric acid, and phosphomolybdate blue methods, respectively, as reported previously.[31–34] The pH of the filtrates was also measured using a pH meter (FE20, METTLER TOLEDO, Switzerland).

Extraction and quantification of CPT and HCPT

After culture for 10 days in the dark, CMCs and DDCs cultures were dried at 55 °C and crushed separately. One gram of the above dried cultures was soaked in 50 mL methanol for 12 h, followed by ultrasonic extraction for 2.5 h. The methanol extracts were centrifuged at 12 000 rpm for 10 min and the supernatants were collected. Then, the residues were extracted with an equal volume methanol twice. The extracts were concentrated and evaporated to dryness. Next, 50 mL of water was added and three extractions were performed using an equal volume of chloroform. The chloroform extracts were evaporated to dryness, dissolved in 3 mL methanol, filtered using a 0.45 μm Acrodisc syringe filter, and analyzed by HPLC. HPLC was performed using a C_{18} column (250 × 4.6 mm, 5 μm; Phenomenex Synergi, USA) with an Agilent 1260HPLC system (Agilent Technologies, Santa Clara, CA, USA) equipped with an ultraviolet detector. The mobile phase consisted of a mixture of MeOH/H_2O (50 : 50, v/v). The flow rate was maintained at 1.0 mL min^{-1}, the injection volume was 10 μL, the detection wavelength was 254 nm, and the column was maintained at 25 °C. The concentrations of CPT and HCPT were determined using standard curves. The standard curves were as follows:

$$CPT, \ Y = 4202.2X - 0.9626 \ (R^2 = 0.9999)$$

$$HCPT, \ Y = 708.86X + 5.5547 \ (R^2 = 0.9992),$$

where Y indicates the peak area of CPT or HCPT and X indicates the concentration of CPT or HCPT.

Expression of CPT and HCPT biosynthesis genes

Plant materials. CMCs and DDCs were separately cultured in solid B_5 medium supplemented with 1.0 mg L^{-1} NAA, 0.5 mg L^{-1} 2,4-D, 0.05 mg L^{-1} KT, 30 g L^{-1} sucrose, and 7.5 g L^{-1} agar at 25 °C in the dark for 10 days for total RNA isolation.

RNA isolation and cDNA synthesis. CMCs and DDCs cultures were ground with a mortar and pestle in liquid nitrogen. Next, 1 mL of Trizol (TaKaRa, Dalian, China) was added to the ground samples, mixed very well, and allowed to settle for 5 min. Then, 0.2 mL of chloroform was added, mixed vigorously for 15 s, settled for 3 min, and centrifuged for 10 min at 12 000 rpm at 4 °C. The supernatants were transferred to new tubes; an equal volume of isopropyl alcohol was added, mixed very well, settled

for 20 min, and centrifuged for 10 min at 12 000 rpm and 4 °C. After removing the supernatant, the precipitates were dissolved in 1 mL of a 3 : 1 ratio of alcohol : DEPC, washed, and centrifuged for 5 min at 12 000 rpm at 4 °C. After removing the supernatant the RNA pellet was air-dried at 25 °C, verified by running on an agarose gel, dissolved in 30 μL of DEPC-treated ddH_2O, and stored at −80 °C. For cDNA synthesis, 1 μg of total RNA was used for reverse transcription using Bestar qPCR RT Kit (DBI, Germany) according to the manufacturer's instructions. Twenty microliters of the cDNA was used as a template for qRT-PCR.

qRT-PCR. Based on the published gene sequences of *IPI*, *G10H*, *ASA1*, *TSB*, *TDC1*, *TDC2*, *STR*, *HMGR2*, and *HMGR3* (GenBank accession numbers DQ839416.1, JF508378.1, AY753655.1, AF042321.1, U73656.1, U73657.2, JF508375.1, U72146.1, and U72145.1, respectively), qRT-PCR primers were designed using Primer 5.0 (Table 1). Gene expression was determined using the relative quantification method with actin (actin-F, 5′-GTGACAATGGAACTGGAATGG-3′; actin-R, 5′-AGACGGAGGATAGCGTGAGG-3′) and 18S (18S-F, 5′-ATGA-TAACTCGACGGATCGC-3′; 18S-R, 5′-CTTGGATGTGG-TAGCCGTTT-3′) as the internal references. For quantification of the standard, the PCR products amplified from cDNA were purified, and their concentration was measured to calculate the number of cDNA copies. qRT-PCR reactions were performed in a 20 μL reaction mixture containing 2 μL template cDNA, 10 μL SYBR Green qPCR Master Mix (DBI, Germany), 0.5 μL of each specific primer (10 μm), and ddH_2O. The thermal cycling conditions were as follows: 95 °C for 2 min, followed by 40 cycles of 94 °C for 20 s, 58 °C for 20 s, and 72 °C for 20 s. The PCR reactions were performed in a Stratagene Mx3000P Real time PCR system (Agilent Technologies, Santa Clara, CA, USA), and the PCR products were analyzed using Bio-Rad CFX Manager 2.0 software. Three replicates per sample were used for the qRT-PCR analysis, and values are expressed as means ± SDs.

Table 1 The primers used for quantitative real-time PCR

Gene names	Primer sequence (5′ to 3′)	Product sizes (bp)
IPI	Forward: AAGGTAACATTCCCTCTGGC	114
	Reverse: CTTCCTTTGTGCAGCATTTC	
G10H	Forward: ATGGATGTATTTATTGCTGCC	141
	Reverse: TTCTACTAACTTGCCTTTGCC	
ASA1	Forward: GGAATGAAACGCTTGGAAAT	111
	Reverse: CTTCAAAGGAGGACCGTAATG	
TSB	Forward: CTGCACTATCGCCAGAGAGAT	175
	Reverse: TTGGTCTCCAGATAGAGATCG	
TDC1	Forward: ACTGAATCTCCGGCATCCGTT	208
	Reverse: TCAGAATGCTCTCGAATGGCT	
TDC2	Forward: AGCGGA ACTTGAGCTGGAGAT	353
	Reverse: CTGCCACGTCAGCTTCTATCT	
STR	Forward: TACCTTTGACTTGCCCCTTG	168
	Reverse: ATTGGTGCTAAGAATGTGTTGTT	
HMGR2	Forward: AGACAAGAAGCCAGCAGCAGT	182
	Reverse: TAAACCCACCAAGAGCACCAG	
HMGR3	Forward: AGGAGGTTGTGAGGAAGGTGT	470
	Reverse: TGATCTGTTGTATTTCATGTGGC	

Conclusions

In the present study, CMCs of *C. acuminata* were isolated for the first time. The characteristic features of *C. acuminate* CMCs, including abundant and small vacuoles within each cell and hypersensitivity to γ-irradiation and zeocin, were consistent with CMCs reported previously. The growth curves and kinetics of CMCs and DDCs were detected simultaneously. Furthermore, HPLC analysis showed that the accumulation of CPT and HCPT was higher in CMCs than DDCs. Additionally, transcriptional analyses determined that the expression of *IPI*, *G10H*, *ASA1*, *TSB*, *TDC1*, *TDC2*, and *STR* was upregulated in CMCs compared with DDCs. The accumulation of CPT and HCPT in CMCs could likely be attributed to the upregulation of these seven genes which offset the effects of *HMGR2* and *HMGR3* downregulation. In conclusion, CMCs may be a good choice for obtaining CPT and HCPT, and this may offer an attractive and cost-effective option for the industrial production of CPT and HCPT.

Acknowledgements

Notes and references

1 M. E. Wall, M. C. Wani, C. E. Cook, K. H. Palmer, A. T. McPhail and G. A. Sim, *J. Am. Chem. Soc.*, 1966, **88**, 3888–3890.

2 Y.-H. Hsiang, R. Hertzberg, S. Hecht and L. F. Liu, *J. Biol. Chem.*, 1985, **260**, 14873–14878.

3 A. Lorence, F. Medina-Bolivar and C. L. Nessler, *Plant Cell Rep.*, 2004, **22**, 437–441.

4 V. J. Venditto and E. E. Simanek, *Mol. Pharmaceutics*, 2010, **7**, 307–349.

5 M. López-Meyer, C. L. Nessler and T. D. McKnight, *Planta Med.*, 1994, **60**, 558–560.

6 K. Sakato, H. Tanaka, N. Mukai and M. Misawa, *Agric. Biol. Chem.*, 1974, **38**, 217–218.

7 A. J. V. Hengel, M. P. Harkes, H. J. Wichers, P. G. M. Hesselink and R. M. Buitelaar, *Plant Cell, Tissue Organ Cult.*, 1992, **28**, 11–18.

8 H. Wiedenfeld, M. Furmanowa, E. Roeder, J. Guzewska and W. Gustowski, *Plant Cell, Tissue Organ Cult.*, 1997, **49**, 213–218.

9 G. Kai, X. Teng, L. Cui, S. Li, X. Hao, M. Shi and B. Yan, *International Journal of Science*, 2014, **3**, 86–95.

10 X. Ni, S. Wen, W. Wang, X. Wang, H. Xu and G. Kai, *J. Appl. Pharm. Sci.*, 2011, **01**, 85–88.

11 W. Wang, Y. Lu, L. Li, J. Wang and G.-Y. Kai, *Acta Bot. Boreali-Occident. Sin.*, 2008, **28**, 2416–2422.

12 C. Frankenstein, D. Eckstein and U. Schmitt, *Dendrochronologia*, 2005, **23**, 57–62.

13 E.-K. Lee, Y.-W. Jin, J. H. Park, Y. M. Yoo, S. M. Hong, R. Amir, Z. Yan, E. Kwon, A. Elfick, S. Tomlinson, F. Halbritter, T. Waibel, B.-W. Yun and G. J. Loake, *Nat. Biotechnol.*, 2010, **28**, 1213–1217.

14 N. Fulcher and R. Sablowski, *Proc. Natl. Acad. Sci. U. S. A.*, 2009, **106**, 20984–20988.

15 B.-W. Yun, Z. Yan, R. Amir, S. Hong, Y.-W. Jin, E.-K. Lee and G. J. Loake, *Biotechnol. Genet. Eng. Rev.*, 2012, **28**, 47–60.

16 T. Furukawa, M. J. Curtis, C. M. Tominey, Y. H. Duong, B. W. L. Wilcox, D. Aggoune, J. B. Hays and A. B. Britt, *DNA Repair*, 2010, **9**, 940–948.

17 R. J. Burnett, I. E. Maldonado-Mendoza, T. D. McKnight and C. L. Nessler, *Plant Physiol.*, 1993, **103**, 41–48.

18 M. López-Meyer and C. L. Nessler, *Plant J.*, 1997, **11**, 1167–1175.

19 H. Lu and T. D. McKnight, *Plant Physiol.*, 1999, **120**, 43–51.

20 H. Lu, E. Gorman and T. D. McKnight, *Planta*, 2005, **221**, 352–360.

21 I. E. Maldonado-Mendoza, R. M. Vincent and C. L. Nessler, *Plant Mol. Biol.*, 1997, **34**, 781–790.

22 X. Pan, M. Chen, Y. Liu, Q. Wang, L. Zeng, L. Li and Z. Liao, *DNA Sequence*, 2008, **19**, 98–105.

23 Y. Sun, H. Luo, Y. Li, C. Sun, J. Song, Y. Niu, Y. Zhu, L. Dong, A. Lv, E. Tramontano and S. Chen, *BMC Genom.*, 2011, **12**, 533–544.

24 S. Kajiwara, P. D. Fraser, K. Kondo and N. Misawa, *Biochem. J.*, 1997, **324**, 421–426.

25 C. A. M. Peebles, G. W. Sander, E. H. Hughes, R. Peacock, J. V. Shanks and K.-Y. San, *Metab. Eng.*, 2011, **13**, 234–240.

26 G. Collu, A. A. Garcia, R. V. D. Heijden and R. Verpoorte, *Plant Sci.*, 2002, **162**, 165–172.

27 Y. Yamazaki, A. Urano, H. Sudo, M. Kitajima, H. Takayama, M. Yamazaki, N. Aimi and K. Saito, *Phytochemistry*, 2003, **62**, 461–470.

28 Q.-Y. Gai, J. Jiao, M. Luo, W. Wang, C.-J. Zhao, Y.-J. Fu and W. Ma, *Ind. Crops Prod.*, 2016, **84**, 350–357.

29 S. J. Hey, S. J. Powers, M. H. Beale, N. D. Hawkins, J. L. Ward and N. G. Halford, *Plant Biotechnol. J.*, 2006, **4**, 219–229.

30 Y.-K. Kim, J. K. Kim, Y. B. Kim, S. Lee, S.-U. Kim and S. U. Park, *J. Agric. Food Chem.*, 2013, **61**, 1928–1934.

31 P. S. Chen, T. Y. Toribara and H. Warner, *Anal. Chem.*, 1956, **28**, 1756–1758.

32 M. Dubois, K. A. Gilles, J. K. Hamilton, P. A. Rebers and F. Smith, *Anal. Chem.*, 1956, **28**, 350–356.

33 U. Hecht and H. Mohr, *Physiol. Plant.*, 1990, **78**, 379–387.

34 M. W. Weatherburn, *Anal. Chem.*, 1967, **39**, 971–974.